Fetal Cells Traffic to Injured Maternal Myocardium and Undergo Cardiac Differentiation

Rina J. Kara, Paola Bolli, Ioannis Karakikes, Iwao Matsunaga, Joseph Tripodi, Omar Tanweer, Perry Altman, Neil S. Shachter, Austin Nakano, Vesna Najfeld and Hina W. Chaudhry

Circulation Research published online November 14, 2011
Circulation Research is published by the American Heart Association. 7272 Greenville Avenue, Dallas, TX 72514
 Print ISSN: 0009-7330. Online ISSN: 1524-4571

Fetal Cells Traffic to Injured Maternal Myocardium and Undergo Cardiac Differentiation

Rina J. Kara, Paola Bolli,* Ioannis Karakikes,* Iwao Matsunaga, Joseph Tripodi, Omar Tanweer, Perry Altman, Neil S. Shachter, Austin Nakano, Vesna Najfeld, Hina W. Chaudhry

Rationale: **Fetal cells enter the maternal circulation during pregnancy and may persist in maternal tissue for decades as microchimeras.**

Objective: **Based on clinical observations of peripartum cardiomyopathy patients and the high rate of recovery they experience from heart failure, our objective was to determine whether fetal cells can migrate to the maternal heart and differentiate to cardiac cells.**

Methods and Results: **We report that fetal cells selectively home to injured maternal hearts and undergo differentiation into diverse cardiac lineages. Using enhanced green fluorescent protein (eGFP)-tagged fetuses, we demonstrate engraftment of multipotent fetal cells in injury zones of maternal hearts. In vivo, eGFP+ fetal cells form endothelial cells, smooth muscle cells, and cardiomyocytes. In vitro, fetal cells isolated from maternal hearts recapitulate these differentiation pathways, additionally forming vascular tubes and beating cardiomyocytes in a fusion-independent manner; ≈40% of fetal cells in the maternal heart express Caudal-related homeobox2 (*Cdx2*), previously associated with trophoblast stem cells, thought to solely form placenta.**

Conclusions: **Fetal maternal stem cell transfer appears to be a critical mechanism in the maternal response to cardiac injury. Furthermore, we have identified *Cdx2* cells as a novel cell type for potential use in cardiovascular regenerative therapy. (*Circ Res*. 2011;109:00-00.)**

Key Words: fetal stem cells ■ microchimerism ■ cardiomyocyte regeneration ■ cardiac repair ■ Cdx2

Microchimerism results when 2 genetically disparate populations of cells appear in the same tissue, organ, or individual.[1] This can be due to transfusion of blood products, organ transplantation, or pregnancy. In this study, we refer to microchimerism derived from the bidirectional trafficking and stable long-term persistence of allogeneic fetal cells in the maternal host, a phenomenon that is common to many Eutheria.[1] Microchimeric cells can modify immunologic recognition or tolerance, affect the course and outcome of various diseases, and demonstrate stem cell–like or regenerative properties.[2]

Fetal-maternal transfer of nucleated cells during pregnancy is a common phenomenon involving multiple cell types, some possessing multilineage potential,[3,4] and these cells appear transiently or persist for decades after delivery in some women.[5] The long-term survival of fetal CD34+ hematopoietic stem/progenitor cells, CD34+ and CD38+ lymphoid progenitors, CD3+ and CD14+ mononuclear cells, CD19+ and IgM+ B lymphocyte precursor cells, CD45+ cells, desmin+ and mesenchymal stem cells have been reported in maternal blood and tissues.[3,5–11] Fetal chimeric progenitor cells have been found in rodent brain,[12] and additionally, fetal cells with regenerative potential have been found in brain, liver, kidney, and lung injuries.[13–15] Fetal cells have also been found to participate in maternal neoangiogenesis during pregnancy at sites of skin inflammation.[16]

To our knowledge, the phenomenon of fetal maternal stem cell transfer has never been explored in the realm of acute cardiac disease. One group has reported that cells of male fetus origin could be found in explanted hearts of 2 women with idiopathic dilated cardiomyopathy many years after a previous pregnancy.[17] This observational study did not determine whether the fetal cells contributed to the development of cardiomyopathy or if their presence represented an attempt at cardiac regeneration. Peripartum cardiomyopathy is known to have the highest recovery rate among all etiologies of heart failure.[18] These clinical observations have led us to hypothesize that fetal or placental cells that enter the maternal

Original received May 20, 2011; revision received September 30, 2011; accepted October 6, 2011. In September 2011, the average time from submission to first decision for all original research papers submitted to *Circulation Research* was 16 days.

From Mount Sinai School of Medicine, Cardiovascular Institute, New York, NY (R.J.K., I.K., P.B., J.T., P.A., V.N., H.W.C.), Columbia University College of Physicians and Surgeons, Division of Cardiology, New York, NY (I.M., O.T., N.S.S.); and UCLA, Department of Molecular, Cell, and Developmental Biology, Los Angeles, CA (A.N.).

*These authors contributed equally to this work.

Correspondence to Hina W. Chaudhry, MD, Cardiovascular Regenerative Medicine, Mount Sinai School of Medicine, One Gustave L. Levy Place, Box 1030, New York, NY 10029. E-mail hina.chaudhry@mssm.edu

Circulation Research **is available at http://circres.ahajournals.org** **DOI: 10.1161/CIRCRESAHA.111.249037**

Non-standard Abbreviations and Acronyms

α-sarc	alpha-sarcomeric actin
α-SMA	alpha-smooth muscle actin
Cdx2	Caudal-related homeobox2
CMFs	cardiac mesenchymal feeders
cTnT	cardiac troponin T
Cx43	connexin 43
eGFP	enhanced green fluorescent protein
ES	embryonic stem
FACS	fluorescence activated cell sorting
MI	myocardial infarction
TS	trophoblast stem
VE-cad	VE-Cadherin
WT	wild-type

circulation may be recruited to the sites of myocardial disease or injury to assist in repair. Identification of the cell types implicated in this process could lead to the development of novel cell therapies for a broader spectrum of cardiovascular disease states. Furthermore, significant controversy exists in the field of stem cell biology as to whether a variety of stem cell types other than embryonic stem (ES) cells, can give rise to beating cardiomyocytes. Our study illustrates that experimental myocardial injury, induced in a pregnant mouse, triggers the flux of fetal cells via the maternal circulation into the injured heart where they undergo differentiation into diverse cardiac cell fates. Fetal cells isolated from the maternal heart undergo clonal expansion and can differentiate into beating cardiomyocytes in vitro. A significant proportion of the fetal cells homing to the heart express Caudal-related homeobox2 (*Cdx2*),[19,20] suggesting for the first time, that trophoblast stem cells are deserving of further investigations for their potential role in organ repair after acute injury.

Methods

An expanded Methods section is available in the Data Supplement at http://circres.ahajournals.org.

Wild-type (WT) B6CBA virgin female mice and enhanced green fluorescent protein (eGPF) transgenic male mice (C57BL/6tg(ACTbeGFP)10sb/J from Jackson Laboratories) were mated and pregnant females subjected to midgestation cardiac injury. All animal care was in compliance with the *Guide for the Care and Use of Laboratory Animals* by the US National Institutes of Health, and institutional guidelines at Mount Sinai School of Medicine.

DNA Extraction

Total DNA was prepared from cells/tissues using the Dneasy mini kit according to manufacturer's instructions (Qiagen, Valencia, CA).

RNA Extraction

Total RNA was extracted from cells/tissue using the Rneasy micro kit (Qiagen, Valencia, CA). cDNA was reverse transcribed from RNA using the SensiScript RT kit (Qiagen, Valencia, CA).

Real-Time Quantitative PCR

Quantitative PCR reactions were performed (SYBR Green Supermix, Biorad, Hercules, CA), using either DNA or cDNA, on the iQ5 Real-Time PCR Detection System (Bio-Rad, Hercules, CA). Fold changes in gene expression were determined using the ΔΔCt method with normalization to either ApoB or GAPDH endogenous controls. Absolute cell numbers for eGFP cells homing to maternal hearts were also assessed.

Immunofluorescence

Maternal heart ventricular sections were fixed and incubated with primary antibody for 1 hour at room temperature, followed by secondary antibody for 1 hour at room temperature and counterstained with DAPI. Sections were then incubated with Sudan black (0.7–70% EtOH) and cover-slipped. See full list of antibodies in Online Supplement Material. Fluorescence in situ hybridization was performed with mouse DNA probes for chromosomes X and Y (see Online Supplement Material for details).

Fluorescence Activated Cell Sorting

Cardiac and skeletal muscle tissue was digested with pronase; solution was filtered through a 70-μm mesh filter to remove residual tissue and underwent several spin cycles to obtain a cell suspension. Cells were sorted utilizing a MoFlo high speed cell sorter (Dako Cytomation, Carpinteria CA). Both eGFP+ (cells of fetal origin) and eGFP− (cells of maternal origin) populations were collected. Data analysis was performed using FlowJo Software (Treestart, Ashland, OR). Analysis of specific cell markers on previously sorted eGFP+ cells was performed with the use of the BD LSR II (BD Biosciences, San Jose, CA). See Online Supplement Material for full antibody list.

Cell Culture

The sorted eGFP+ fetal cells were cultured on cardiac mesenchymal feeders (CMFs) and on neonatal cardiomyocytes. Live cell imaging was performed using an Olympus IX-70 Live cell imaging system (Olympus, Center Valley, PA).

Data Analysis

Statistical analysis was performed with the Student's *t* test.

Results

Fetal Cells Home to and Engraft in Injured Maternal Myocardium

WT virgin female mice, age 3–6 months, were crossed with heterozygous eGFP transgenic male mice. The female mice underwent ligation of the left anterior descending artery in order to induce an anterolateral myocardial infarction (MI) at gestation day 12 (Figure 1A). Consistent with our previous work, this results in approximately 50% left ventricular infarction.[21] In accordance with Mendelian autosomal inheritance, approximately 50% of embryos were eGFP+.

Initially, we quantified eGFP expression in injured maternal hearts relative to sham-operated pregnant mice and controls in which no injury was induced. Postpartum females were euthanized at 1 or 2 weeks after MI. Total DNA was extracted from each total heart and eGFP expression analyzed[22] (Figure 1B). Infarcted hearts harvested at 1 week after MI contained 120 times more eGFP than

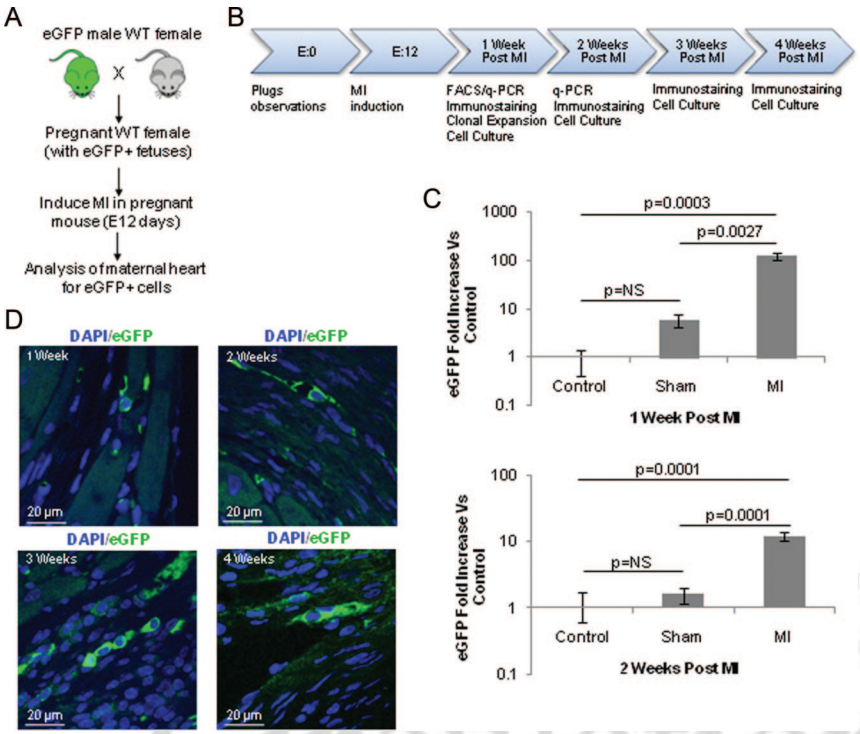

Figure 1. Experimental model and tracking of eGFP+ fetal cells in maternal heart. A, Schematic of the experimental protocol. **B**, Mice were killed at several time points for molecular and cellular analyses to track eGFP+ cells in maternal hearts and to assess their differentiation pathways. **C**, Quantitative PCR demonstrates significantly greater levels of eGFP expression in pregnant mice subjected to cardiac injury (1 wk = 120.0±17.0; 2 wks = 12.0±1.6; n=3) compared with shams (1 wk = 6.0±1.7; 2 wks = 1.6±0.4; n=3) and noninfarcted controls (1 wk = 1.0±0.6; 2 wks = 1.0±0.7; n=3). Error bars are SEM. **D**, Ventricular sections from maternal hearts analyzed at 1, 2, 3, and 4 wks postinjury illustrate eGFP+ cells engrafting within infarct and periinfarct zones. Fetal cells are positive for eGFP (bright green), nuclei are stained with DAPI, and light green background fluorescence is noted in maternal cardiomyocytes.

controls (P=0.0003) and 20 times more eGFP than shams (P=0.0027). Infarcted hearts harvested at 2 weeks after MI contained 12 times more eGFP than controls (P=0.0001) and 8 times more eGFP than shams (P=0.0001) (Figure 1C). The absolute numbers of eGFP cells in control, sham-operated, and MI hearts were also computed based on quantitative PCR (Online Table I), and 1.7% of the total heart at 2 weeks after injury was composed of eGFP cells.

Fetal Cells Adopt Diverse Cardiac Lineages In Vivo

In a separate group of infarcted and control mice, immunofluorescence analysis with confocal microscopy was utilized to detect eGFP+ cells in ventricular tissue sections of maternal hearts at various time points subsequent to myocardial injury (Figure 1B and 1D). EGFP+ cells were noted in infarct zones and peri-infarct zones of infarcted maternal hearts at 1, 2, 3, or 4 weeks after MI (Figure 1D and Online Table II, A). Negligible numbers of eGFP cells were noted in noninfarct zones of the infarcted maternal hearts (Online Table II, B). We further sought to determine whether the eGFP+ cells were differentiating into more mature cardiac cells as we noted a decrease in nuclear to cytoplasmic ratio with an increase in postinjury time (Figure 1D). At 3 and 4 weeks after MI, eGFP+ cells observed in the infarct zones of maternal hearts also expressed markers of cardiomyocytes (α-sarcomeric actin and α-actinin), smooth muscle cells (α-smooth muscle actin), and endothelial cells (CD31 and VE-cadherin) (Figure 2A). At 3 weeks after MI, 50% of all eGFP-positive nuclei belonged to cells that also stained positive for α-actinin, implying that 50% of eGFP cells homing to the heart may have differentiated to cardiomyocytes (Online Table II, C). These results suggest that fetal cells differentiated into diverse lineages within maternal cardiac tissue.

Spectral profiles were obtained from paraffin-embedded ventricular tissue sections of infarcted maternal hearts. This measure was taken, in addition to the use of Sudan black, to ensure that native autofluorescence of cardiomyocytes was not affecting fluorescence images. A representative section is depicted in Figure 2B, and the mean intensities of the spectral scans for this section are plotted versus wavelength in Figure 2C. The mean intensities of the sample regions are significantly higher than the mean intensities of the control regions.

Fetal Cells Isolated From Injured Maternal Hearts Differentiate to Endothelial Cells, Smooth Muscle Cells, and Spontaneously Beating Cardiomyocytes In Vitro

We next used fluorescence activated cell sorting (FACS) to isolate fetal eGFP+ cells that had homed to maternal hearts and analyzed their in vitro behavior. When plated on CMFs, we noted clonal expansion of the fetal cells (Figure 3A), their differentiation into smooth muscle cells (Figure 3B) and endothelial cells (Figure 3B), and the formation of vascular structures (Figure 3A and 3C). Other unidentified cellular phenotypes were also observed in these in vitro experiments with CMFs (data not shown). Because we did not observe differentiation of fetal cells into cardiomyocytes on CMFs, we used cardiomyocytes isolated from neonatal cyclin A2 transgenic mice[21] as feeders. When plated on these feeders with standard medium consisting of

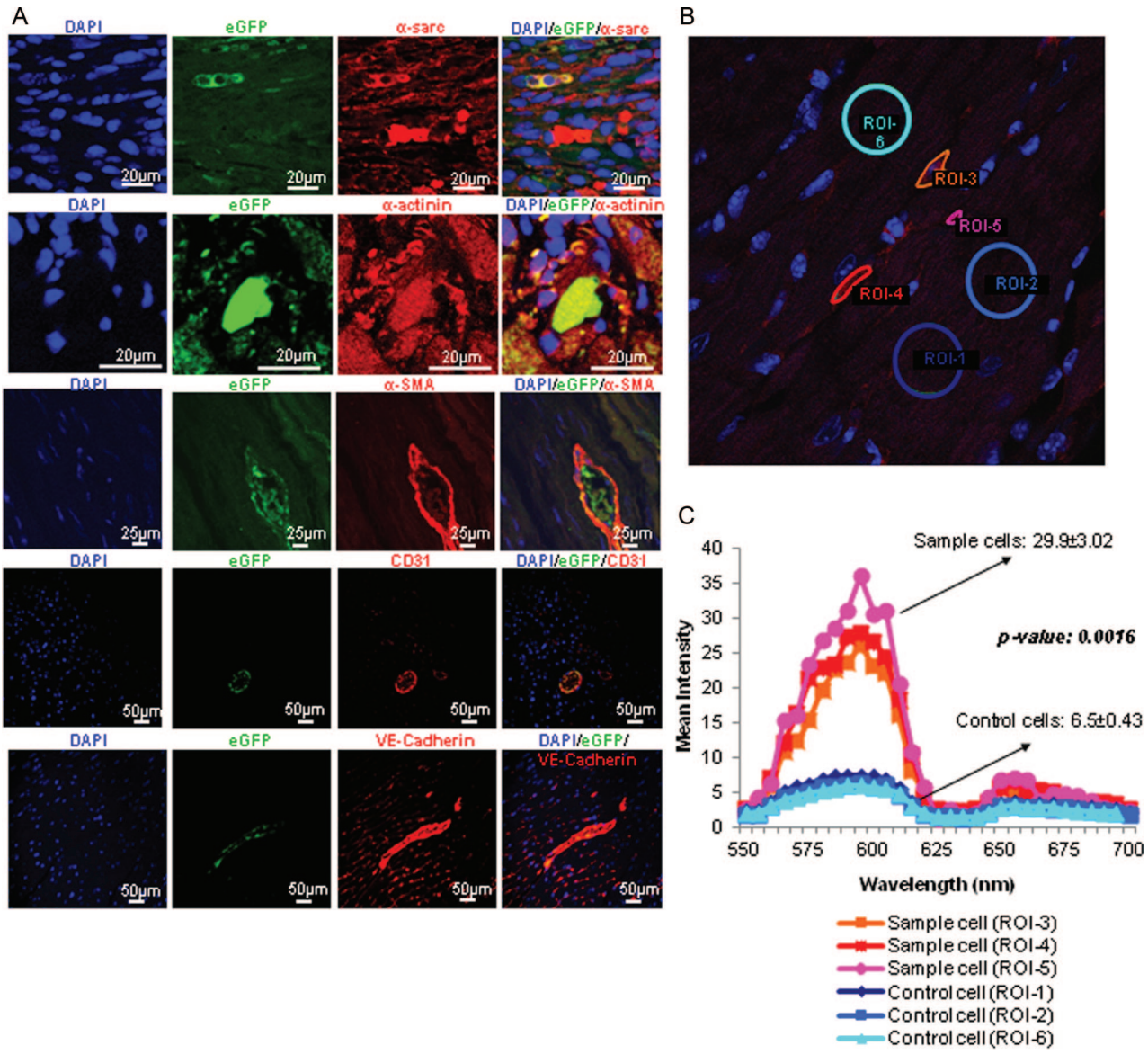

Figure 2. Fetal cells differentiate into diverse cardiac lineages after homing to maternal heart. A, In vivo analysis demonstrates that fetal cells (eGFP+) differentiate into cardiomyocytes expressing α-sarcomeric actin (α-sarc) and α-actinin, smooth muscle cells expressing α-smooth muscle actin (α-SMA), and endothelial cells expressing CD31 and VE-cadherin (VE-cad). **B**, Paraffin-embedded ventricular sections obtained from infarcted hearts of pregnant mice 1 wk after injury; stained with rabbit anti-GFP primary antibody and donkey anti-rabbit Alexa Fluor 568 secondary antibody. Circled regions represent regions of interest (ROIs) 1–6 that were subjected to spectral scanning. **C**, Mean intensities of the spectral profiles from ROIs 1–6, where ROI 1, 2, and 6 are control areas and ROI 3, 4, and 5 represent eGFP+ cells.

DMEM supplemented with FBS, the isolated eGFP+ fetal cells differentiated into spontaneously beating cardiomyocytes (≈48 bpm, Figure 3D and Online Supplement Movies SI, SIA, Movie Still Image SIB, and Movies SII and SIII). The resulting lineages also expressed cardiac troponin T (Figure 3E). Further analysis of eGFP+ fetal cells cultured for 5 weeks in chamber slides indicated expression of the gap junction marker connexin 43 (Figure 3E). This provides compelling evidence for formation of electromechanical connections between the cardiomyocytes derived from eGFP+ fetal cells and the feeder cardiomyocytes.

Fetal Cells Exhibit Clonality and Undergo Cardiac Differentiation in a Fusion-Independent Manner

Clonal analysis was performed to confirm the "stemness" of the fetal cells giving rise to cardiac cells (Figure 4A). FACS for eGFP+ cells was performed and single cells were seeded in 96-well plates containing WT neonatal cardiomyocytes as feeders. Clones derived from eGFP+ fetal cells were expanded for 14 days and total clones counted in each colony. Two 96-well plates were used, and 4 wells in each plate gave rise to colonies after 7 days (approximately 50% of the wells in each plate contained

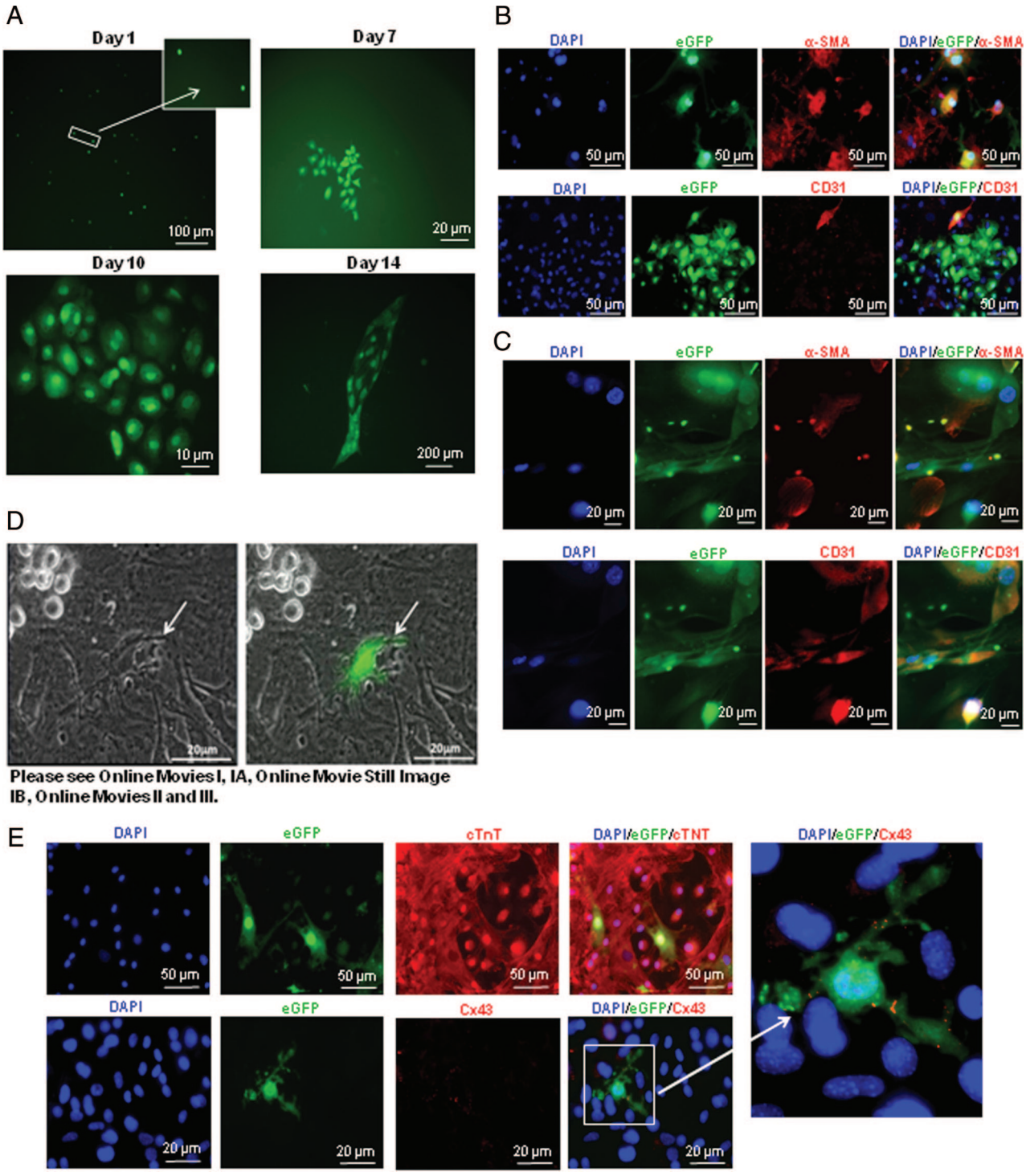

Figure 3. In vitro behavior of eGFP+ cells isolated from maternal hearts. A, In vitro analysis of fetal cells isolated from maternal hearts demonstrates clonal expansion on CMFs. 14 days after plating, vascular tube formation is noted in a 3-dimensional collagen matrix. **B**, Fetal cells isolated from maternal hearts and plated on CMFs undergo differentiation into smooth muscle cells (α-SMA) and endothelial cells (CD31). **C**, Vascular tube formation is noted from fetal cells isolated from maternal hearts and plated on CMFs with expression of α-SMA and CD31. **D**, Fetal cells isolated from maternal hearts and plated on cyclin A2 neonatal cardiomyocytes differentiate into beating cardiomyocytes (Online Movies I, IA, Online Movie still image IB, and Online Movies II and III). **E**, Cardiomyocytes arising from fetal cells isolated from maternal hearts express cardiac troponin T (cTnT) and connexin 43 (Cx43).

viable cells at this time point), yielding an approximate cloning efficiency of 8.3%.

To mechanistically assess whether fusion rather than differentiation was the cause of the appearance of eGFP+ cardiomyocytes in our in vitro assays, we analyzed the number of nuclei present within our fetal cell-derived cardiomyocytes and consistently noted that these cardiomyocytes were mononuclear (Figure 4B). In the first 2 panels of Figure

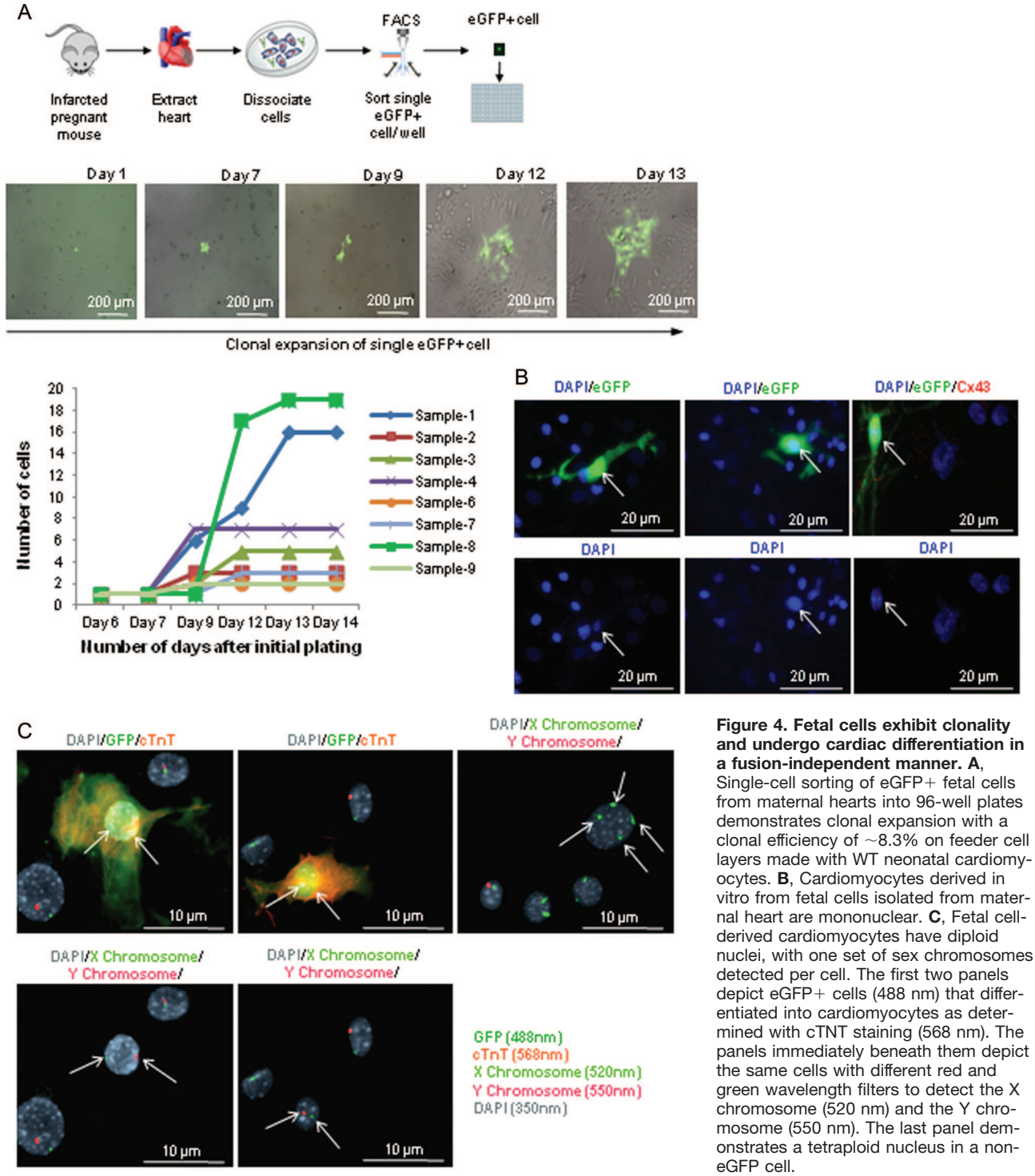

Figure 4. Fetal cells exhibit clonality and undergo cardiac differentiation in a fusion-independent manner. A, Single-cell sorting of eGFP+ fetal cells from maternal hearts into 96-well plates demonstrates clonal expansion with a clonal efficiency of ~8.3% on feeder cell layers made with WT neonatal cardiomyocytes. **B**, Cardiomyocytes derived in vitro from fetal cells isolated from maternal heart are mononuclear. **C**, Fetal cell-derived cardiomyocytes have diploid nuclei, with one set of sex chromosomes detected per cell. The first two panels depict eGFP+ cells (488 nm) that differentiated into cardiomyocytes as determined with cTNT staining (568 nm). The panels immediately beneath them depict the same cells with different red and green wavelength filters to detect the X chromosome (520 nm) and the Y chromosome (550 nm). The last panel demonstrates a tetraploid nucleus in a non-eGFP cell.

4B, where only GFP and DAPI staining is seen, still pictures were taken from the Online Supplementary Movies that accompany this manuscript depicting the beating of these cells (Online Movies II and III). Furthermore, fluorescence in situ hybridization (FISH) for X- and Y-chromosomes revealed 1 set of sex chromosomes within the eGFP+ cardiomyocyte nuclei, establishing the diploid nature of these nuclei and effectively ruling out fusion between eGFP+ fetal cells and feeder cardiomyocytes as the source of eGFP+ cardiomyocytes (Figure 4C). The panels immediately beneath each figure depict only the nuclei of the cells, and as the X, Y probes exhibit fluorescence at different wavelengths (FITC: 520 nm, Cy3: 550 nm, respectively), their signals can be easily distinguished from the green fluorescence of the GFP (Alexa 488: 488 nm) and the secondary antibody to cardiac troponin T (Texas Red: 568 nm). The ease of detecting tetraploid nuclei with this assay is shown in the last panel of Figure 4C depicting cells that were found in a region where GFP cells were not detected.

Fetal Cells Selectively Home to the Injured Maternal Heart and Not to Noninjured Organs

To assess whether eGFP+ cells from the fetus were homing selectively to the injured heart, we used FACS to sort eGFP+ cells from a variety of organs and tissues harvested from pregnant mice subjected to cardiac injury. These organs and tissues were minced and triturated to generate cell suspensions (Figure 5A). Corresponding cell populations were obtained from age-matched pregnant WT female mice mated with WT males and used as controls to establish the appropriate FACS gates to select eGFP+ cells. Cells were isolated from the injured heart, blood, skeletal muscle, chest wall, eGFP− littermates, liver, lung, and placenta. FACS to select eGFP+ cells was performed at 2 time points, 4.5 days after injury (before delivery) and 7 days after injury (after delivery) for all of these tissues except placenta (analyzed before delivery only) as it is resorbed by the mother in mice at time of delivery (Figure 5B). The low quantity of eGFP+ cells in all tissues, including injured heart, before 4.5 days after injury precluded any detailed phenotypic analyses. Therefore, it appears that mobilization of fetal cells in response to maternal injury takes approximately 4.5 days. In the injured heart, ≈1.1% of the cells were eGFP+ before delivery and this number rose significantly to ≈6.3% just after delivery. In blood, ≈1.3% of cells were eGFP+ before delivery and this number rose to ≈3.6% after delivery, although this increase was not statistically significant. Delivery therefore seems to cause the numbers of fetal cells entering the maternal circulation to rise, and this corresponds with a significant increase in fetal cells homing to the injured heart. There were negligible numbers of eGFP+ cells noted in skeletal muscle before and after delivery. The chest wall, where a lesser degree of injury was induced as an incision had to be performed to induce cardiac injury, exhibited a relatively smaller percentage of fetal cells compared with heart and blood. There was no increase in the number of fetal cells homing to the chest wall after delivery, likely due to healing in the 7 days after injury. EGFP− littermates were also examined for the presence of eGFP+ cells. Although a few cells were noted before delivery, probably as the result of the shared circulation with the eGFP+ littermates, eGFP cells were not detected in these littermates after delivery. Liver and lung exhibited negligible numbers of fetal cells. As expected, placenta exhibited the largest percentage of eGFP cells with approximately 36% of placenta cells expressing eGFP. Overall, the results provide clear evidence for the selective and specific homing of eGFP+ fetal cells to the injured heart of the mother, and not to other noninjured maternal tissues (Figure 5B).

Fetal Cells Isolated From Maternal Hearts Express a Variety of Progenitor Markers, Most Notably Cdx2

To establish the identity of the cell type(s) involved in fetal maternal transfer, we analyzed FACS-sorted, eGFP+ cells isolated from maternal hearts 1 week after injury for stem/progenitor cell markers (Figure 6A). 80% of these cells expressed *Nkx2.5*,[23–25] implying that cardiomyogenic differentiation had begun as soon as these cells entered the injured maternal heart. Consistent with this, negligible expression of *Nkx2.5* was found in eGFP+ cells isolated from end-gestation placentas from mice that had undergone cardiac injury (Online Table IV and Online Figure I). Additionally, 46% of cells homing to the maternal heart expressed CD31,[26,27] which was not surprising given the degree of fetal cell-mediated vasculogenesis we observed in injured maternal hearts. The next most common marker found was *Cdx2* (38% of fetal cells). *Cdx2* regulates trophoblast stem (TS) cell development and proliferation[19,20] and has never previously been associated with cardiomyogenic differentiation. The latter finding raises the possibility that in the setting of acute injury, TS cells from placenta can give rise to various cardiac lineages in addition to forming placenta. Fetal cells isolated from maternal hearts also displayed lower levels of several markers of endogenous cardiac progenitors, namely Sca-1[28,29] (21%), cKit[30] (25%) and Islet1[31] (3%), as well as ES cell markers *Pou5f1* (2%), *Nanog* (3%), and *Sox2* (24%).[32,33] The higher expression of *Sox2* is consistent with its expression in non-ES cells as well. Finally, hematopoietic stem cell factor CD34[34,35] was expressed in 15% of the eGFP+ cells, which was not surprising as the placenta is a rich source of hematopoietic stem cells[36] (Figure 6A).

As the eGFP+ cells were traversing through or derived from the placenta, we analyzed gene expression of known "stemness" factors in eGFP+ cells. We sorted eGFP+ cells from end-gestation placentas from three different pregnant mice that had been subjected to myocardial injury. RNA expression of 92 known pluripotency genes was analyzed (Online Table III), and gene expression relative to GAPDH expression for the most prevalent transcripts is plotted in Figure 6B. These mRNA array studies confirmed the presence of *Cdx2* and Eomesodermin (*Eomes*),[20] another marker of TS cells, in the eGFP+ placenta cells.

Discussion

The selective homing of eGFP+ cells in our model to the site of maternal cardiac injury with lack of such homing to noninjured tissues points to the presence of precise signals sensed by cells of fetal origin that enable them to target diseased myocardium specifically and to differentiate into diverse cardiac lineages (Figure 7). Most notable is their differentiation into functional cardiomyocytes that are able to beat in syncytium with neighboring cardiomyocytes (Online Movie I, IA, and Movie Still Image IB), thus potentially uncovering an evolutionary mechanism whereby the fetus assists in protecting the mother's heart during and after pregnancy. These studies were inspired by the recovery noted in peripartum cardiomyopathy, whereby a remarkable 50% of women recover from heart failure spontaneously.[37–39] Peripartum cardiomyopathy has the highest rate of recovery among all etiologies of heart failure,[18] and the reasons for this high rate of recovery are not understood. In fact, it was this very observation that prompted us to hypothesize that there might be a fetal or placental contribution to counteract

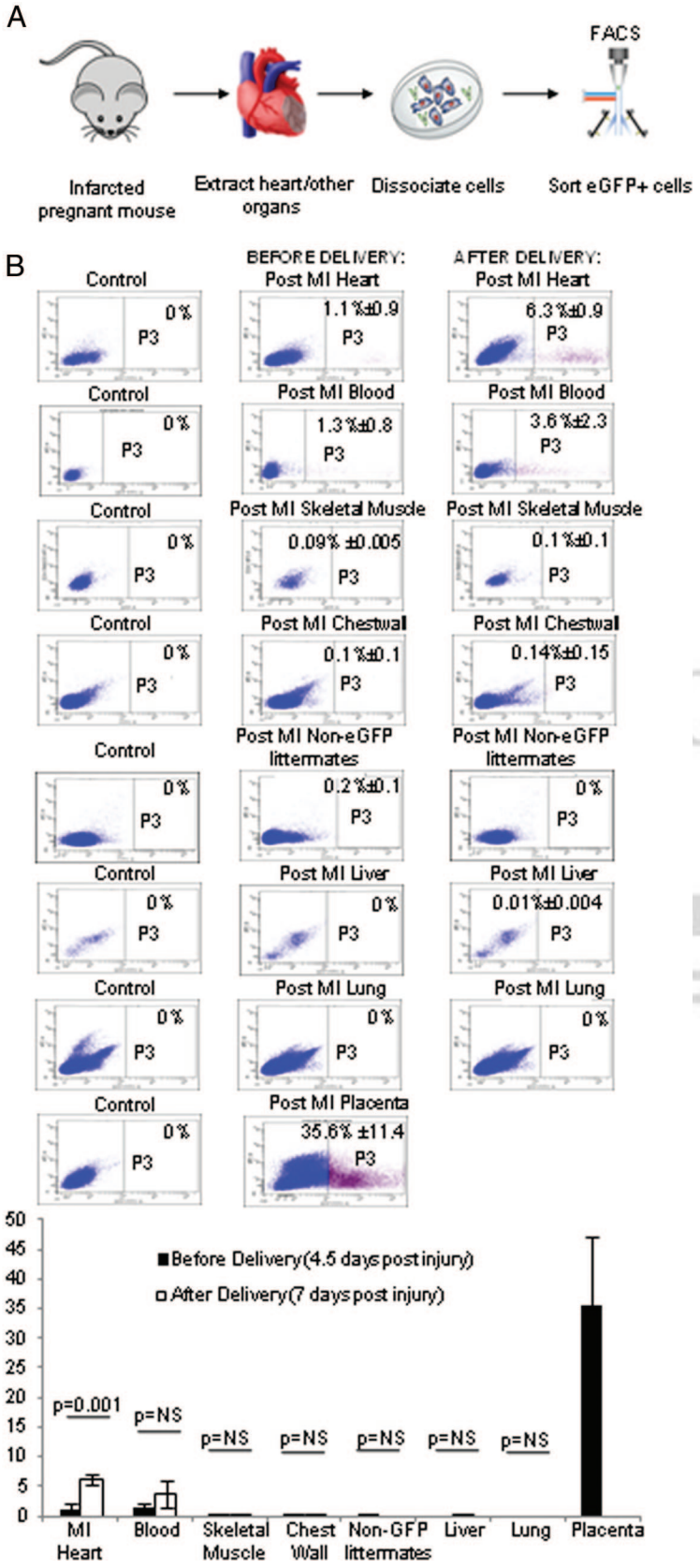

Figure 5. Fetal cells selectively home to injured maternal hearts and not to noninjured organs and express various stem cell markers, including *Cdx2*. **A**, eGFP+ cells were sorted from cell suspensions prepared from various organs and tissues. **B**, Fetal cell numbers in injured heart and blood increased immediately after delivery. Representative FACS profiles are shown for eGFP+ cell sorting from injured heart and blood and noninjured organs with mean percentages of eGFP+ cells (minimum, n=3). Mean percentages of fetal cells plus SEM plotted for each organ as follows: MI heart = 1.10±0.90 before delivery (n=10) and 6.32±0.90 after delivery (n=19), P=0.001; blood = 1.34±0.81 before delivery (n=10) and 3.59±2.30 after delivery (n=15) P=NS; placenta = 35.6±11.47 after delivery (n=3). Very low to undetectable numbers are found for all other organs.

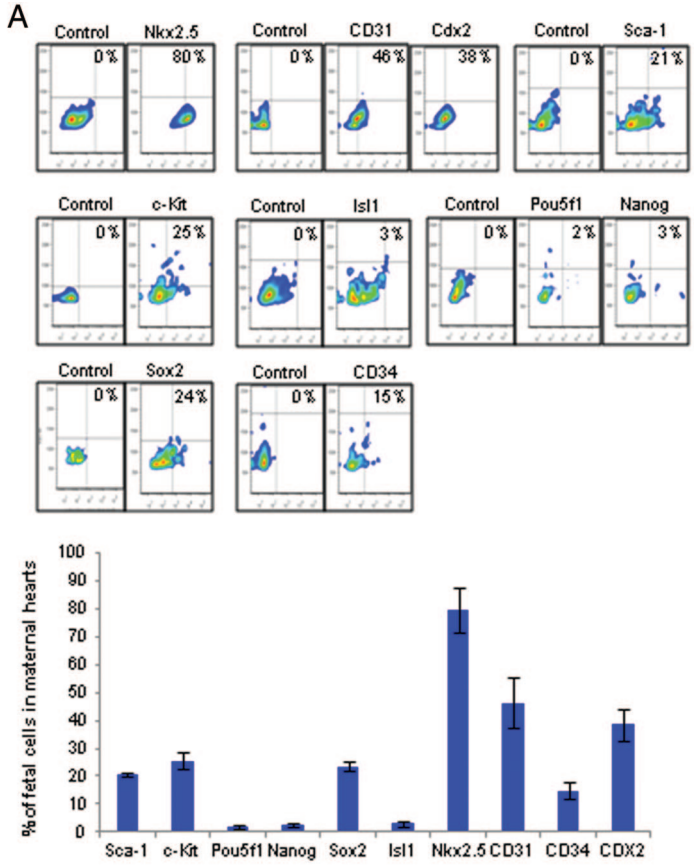

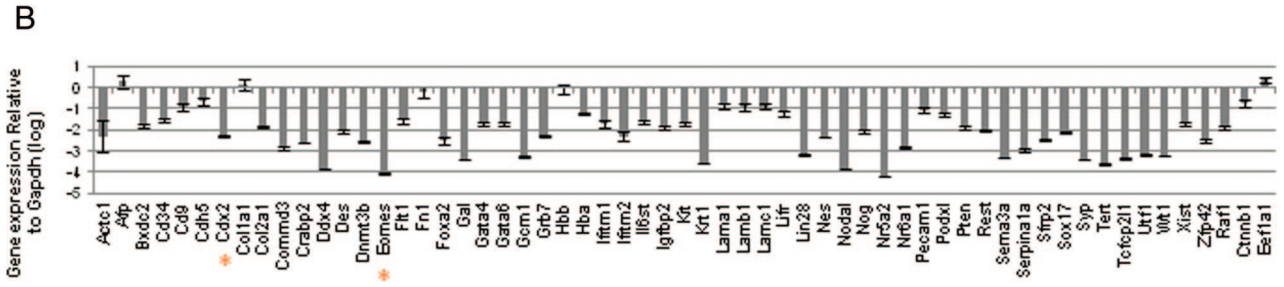

Figure 6. Fetal cells selectively homing to injured maternal hearts express various stem cell markers, including *Cdx2.* A, eGFP+ fetal cells were sorted from maternal hearts 1 wk after injury. By using FACS analysis, we quantitated percentages of eGFP+ cells expressing various stem/progenitor cell surface markers and transcription factors. Quantitation for each marker was performed in triplicate, and mean percentage plus SEM was plotted as follows: Nkx2.5 79.69±8.08; CD31 46.40±8.77; Cdx2 38.39±5.70; Sca-1 20.73±0.80; c-Kit 25.39±2.99; Islet1 2.99±0.97; Pou5f1 1.97±0.82; Nanog 2.72±0.49; Sox2 23.52±1.85; CD34 14.90±2.97. **B**, eGFP+ cells were sorted from end-gestation placentas from 3 pregnant mice subjected to myocardial injury. RNA expression array of 92 pluripotency genes was performed; gene expression relative to GAPDH is plotted for genes with the highest expression levels. Of note, TS cell markers *Cdx2* and *Eomes* are among genes with highest expression.

maternal cardiac injury. Our mouse injury model is not a precise representation of peripartum cardiomyopathy, rather, it is a model system of murine fetomaternal microchimerism that can help identify appropriate cell types for cardiac regeneration.

To this end, a far greater spectrum of potential applications to the field of heart disease emerges from these studies. The challenge of cardiovascular regenerative medicine is to develop novel therapeutic strategies to facilitate regeneration of normally functioning cardiomyocytes in the diseased heart. Thus, many investigators have explored a myriad of approaches in the last decade, many of which we have recently reviewed.[40] Despite investigations with a wide variety of cell types as candidates to attain this goal, the results of stem cell transplantation are somewhat ambiguous and the ideal cell type has yet to be established. The use of bone marrow cells to regenerate infarcted myocardium has been investigated in numerous studies since the initial findings of Orlic et al.[41] Currently, however, a consensus has emerged that the ability of bone marrow–derived stem cells to differentiate into cardiomyocytes is questionable. Less controversy surrounds evidence from several groups demonstrating that ES cells[42–45] and endogenous populations of cardiac stem cells[28,30,31,46,47] have replicative and potentially regenerative capacities. Despite promising results with ES cells, there are ethical issues regarding the use of embryonic material as well as the tendency of ES cells to form teratomas.[42] Native cardiac progenitors, left in their natural milieu at their naturally occurring frequency, are clearly inadequate in reversing the downward spiral of events culminating in heart failure. Many of these progenitor types have not been reported to differentiate to functional beating cardiomyocytes when tested ex vivo. Utilizing live imaging, we have demonstrated that fetal cells differentiate into spontaneously beating cardiomyocytes after homing to the heart. The demonstration of spontaneous beating ex vivo has been a major stumbling block in the field. Coculture with neonatal cardiomyocytes was necessary in our study to induce beating, but we did not find any

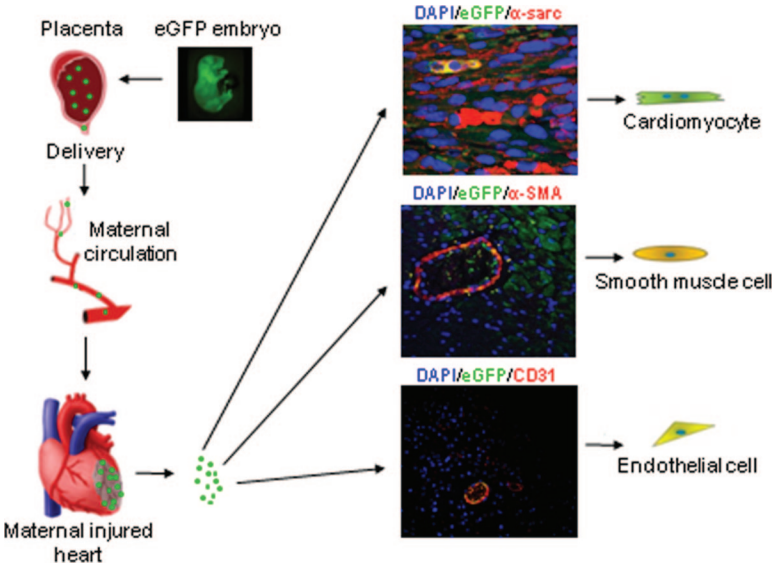

Figure 7. Model depicting trafficking of cells from fetus across placenta into maternal circulation to injury and periinjury zones of the maternal heart. Cells of fetal origin engraft within maternal heart and give rise to diverse cardiac lineages, including cardiomyocytes, smooth muscle cells, and endothelial cells.

examples of nuclear fusion among the cardiomyocytes that were also GFP-positive. We cannot rule out "transient cell fusion" as described by Dimmeler et al,[48] but they noted that the nanotubular structures underlying these intercellular connections had declined by 48 hours after coculture. We did not observe any beating GFP+ cells until at least 4 weeks after coculture, implying that true differentiation took place. Further studies and perhaps novel methods are needed to surmount these challenges in ascertaining true differentiation.

Our identification of *Cdx2* as a unique and highly prevalent marker expressed on fetal cells in the maternal myocardium offers a new perspective regarding the appropriate cell type that might achieve these aims. The Cdx family of transcription factors consists of 3 mouse homologues (*Cdx 1, 2*, and *4*) of the *Drosophila* caudal homeobox genes, which are involved in specifying cell position along the anteroposterior axis, with similar functions in the later developmental stages of the mouse embryo[20,49] as well as morphological specification of murine gut endoderm.[50,51] *Cdx2* is also required for trophectoderm fate commitment in the developing blastocyst.[19,20,52] The trophectoderm gives rise to the trophoblast stem cells which have previously been associated solely with differentiation to the placenta lineage.[53,54]

Bianchi et al found that fetal cells that traffic to maternal blood and organs comprise a mixed population of progenitor and differentiated cells, with different relative proportions in different maternal organs[3] in a study that was performed in the noninjured state. In accordance with prior studies demonstrating a variety of different phenotypes in fetal microchimeric cells, our results also point toward the transfer of several populations of progenitor cells, but our finding of *Cdx2* cells of fetal or placental origin in the heart may have uncovered a novel cell type that is capable of cardiac differentiation under injury conditions that can be readily isolated from placenta.

Acknowledgments

We thank I. Lemischka, D. Wolgemuth, and M. Zaide for critical review of the data and manuscript; R. Huq, V. Friedrich, and the Mount Sinai Microscopy Shared Resource Facility for assistance with spectral profiling; and X. Qiao and the Mount Sinai Flow Cytometry Shared Resource Facility for technical assistance.

Sources of Funding

This work was supported by National Institutes of Health grant (R01-HL 088255).

Disclosures

None.

References

1. Liegeois A, Escourrou J, Ouvre E, Charreire J. Microchimerism: a stable state of low-ratio proliferation of allogeneic bone marrow. *Transplant Proc*. 1977;9:273–276.
2. Klonisch T, Drouin R. Fetal-maternal exchange of multipotent stem/progenitor cells: microchimerism in diagnosis and disease. *Trends Mol Med*. 2009;15:510–518.
3. Fujiki Y, Johnson KL, Peter I, Tighiouart H, Bianchi DW. Fetal cells in the pregnant mouse are diverse and express a variety of progenitor and differentiated cell markers. *Biol Reprod*. 2009;81:26–32.
4. Khosrotehrani K, Johnson KL, Cha DH, Salomon RN, Bianchi DW. Transfer of fetal cells with multilineage potential to maternal tissue. *JAMA*. 2004;292:75–80.
5. Bianchi DW, Zickwolf GK, Weil GJ, Sylvester S, DeMaria MA. Male fetal progenitor cells persist in maternal blood for as long as 27 years postpartum. *Proc Natl Acad Sci U S A*. 1996;93:705–708.
6. Campagnoli C, Roberts IA, Kumar S, Bennett PR, Bellantuono I, Fisk NM. Identification of mesenchymal stem/progenitor cells in human first-trimester fetal blood, liver, and bone marrow. *Blood*. 2001;98:2396–2402.
7. Khosrotehrani K, Leduc M, Bachy V, Nguyen Huu S, Oster M, Abbas A, Uzan S, Aractingi S. Pregnancy allows the transfer and differentiation of fetal lymphoid progenitors into functional t and b cells in mothers. *J Immunol*. 2008;180:889–897.
8. Mikhail MA, M'Hamdi H, Welsh J, Levicar N, Marley SB, Nicholls JP, Habib NA, Louis LS, Fisk NM, Gordon MY. High frequency of fetal cells within a primitive stem cell population in maternal blood. *Hum Reprod*. 2008;23:928–933.

9. Nguyen Huu S, Dubernard G, Aractingi S, Khosrotehrani K. Feto-maternal cell trafficking: a transfer of pregnancy associated progenitor cells. *Stem Cell Rev*. 2006;2:111–116.
10. O'Donoghue K, Choolani M, Chan J, de la Fuente J, Kumar S, Campagnoli C, Bennett PR, Roberts IA, Fisk NM. Identification of fetal mesenchymal stem cells in maternal blood: implications for non-invasive prenatal diagnosis. *Mol Hum Reprod*. 2003;9:497–502.
11. Osada H, Doi S, Fukushima T, Nakauchi H, Seki K, Sekiya S. Detection of fetal hpcs in maternal circulation after delivery. *Transfusion*. 2001;41: 499–503.
12. Tan XW, Liao H, Sun L, Okabe M, Xiao ZC, Dawe GS. Fetal microchimerism in the maternal mouse brain: a novel population of fetal progenitor or stem cells able to cross the blood-brain barrier? *Stem Cells*. 2005;23:1443–1452.
13. Chen J, Sanberg PR, Li Y, Wang L, Lu M, Willing AE, Sanchez-Ramos J, Chopp M. Intravenous administration of human umbilical cord blood reduces behavioral deficits after stroke in rats. *Stroke*. 2001;32: 2682–2688.
14. Kleeberger W, Versmold A, Rothamel T, Glockner S, Bredt M, Haverich A, Lehmann U, Kreipe H. Increased chimerism of bronchial and alveolar epithelium in human lung allografts undergoing chronic injury. *Am J Pathol*. 2003;162:1487–1494.
15. Wang Y, Iwatani H, Ito T, Horimoto N, Yamato M, Matsui I, Imai E, Hori M. Fetal cells in mother rats contribute to the remodeling of liver and kidney after injury. *Biochem Biophys Res Commun*. 2004;325: 961–967.
16. Nguyen Huu S, Oster M, Uzan S, Chareyre F, Aractingi S, Khosrotehrani K. Maternal neoangiogenesis during pregnancy partly derives from fetal endothelial progenitor cells. *Proc Natl Acad Sci U S A*. 2007;104: 1871–1876.
17. Bayes-Genis A, Bellosillo B, de la Calle O, Salido M, Roura S, Ristol FS, Soler C, Martinez M, Espinet B, Serrano S, Bayes de Luna A, Cinca J. Identification of male cardiomyocytes of extracardiac origin in the hearts of women with male progeny: male fetal cell microchimerism of the heart. *J Heart Lung Transplant*. 2005;24:2179–2183.
18. Felker GM, Thompson RE, Hare JM, Hruban RH, Clemetson DE, Howard DL, Baughman KL, Kasper EK. Underlying causes and long-term survival in patients with initially unexplained cardiomyopathy. *N Engl J Med*. 2000;342:1077–1084.
19. Niwa H, Toyooka Y, Shimosato D, Strumpf D, Takahashi K, Yagi R, Rossant J. Interaction between oct3/4 and cdx2 determines trophectoderm differentiation. *Cell*. 2005;123:917–929.
20. Strumpf D, Mao CA, Yamanaka Y, Ralston A, Chawengsaksophak K, Beck F, Rossant J. Cdx2 is required for correct cell fate specification and differentiation of trophectoderm in the mouse blastocyst. *Development*. 2005;132:2093–2102.
21. Cheng RK, Asai T, Tang H, Dashoush NH, Kara RJ, Costa KD, Naka Y, Wu EX, Wolgemuth DJ, Chaudhry HW. Cyclin a2 induces cardiac regeneration after myocardial infarction and prevents heart failure. *Circ Res*. 2007;100:1741–1748.
22. Pfaffl MW. A new mathematical model for relative quantification in real-time RT-PCR. *Nucleic Acids Res*. 2001;29:e45.
23. Komuro I, Izumo S. Csx: A murine homeobox-containing gene specifically expressed in the developing heart. *Proc Natl Acad Sci U S A*. 1993;90:8145–8149.
24. Lints TJ, Parsons LM, Hartley L, Lyons I, Harvey RP. Nkx-2.5: A novel murine homeobox gene expressed in early heart progenitor cells and their myogenic descendants. *Development*. 1993;119:969.
25. Ueyama T, Kasahara H, Ishiwata T, Nie Q, Izumo S. Myocardin expression is regulated by nkx2.5, and its function is required for cardiomyogenesis. *Mol Cell Biol*. 2003;23:9222–9232.
26. Albelda SM, Muller WA, Buck CA, Newman PJ. Molecular and cellular properties of pecam-1 (endocam/cd31): a novel vascular cell-cell adhesion molecule. *J Cell Biol*. 1991;114:1059–1068.
27. Newman PJ, Berndt MC, Gorski J, White GC II, Lyman S, Paddock C, Muller WA. Pecam-1 (cd31) cloning and relation to adhesion molecules of the immunoglobulin gene superfamily. *Science*. 1990;247: 1219–1222.
28. Oh H, Bradfute SB, Gallardo TD, Nakamura T, Gaussin V, Mishina Y, Pocius J, Michael LH, Behringer RR, Garry DJ, Entman ML, Schneider MD. Cardiac progenitor cells from adult myocardium: homing, differentiation, and fusion after infarction. *Proc Natl Acad Sci U S A*. 2003;100: 12313–12318.
29. Oh H, Chi X, Bradfute SB, Mishina Y, Pocius J, Michael LH, Behringer RR, Schwartz RJ, Entman ML, Schneider MD. Cardiac muscle plasticity in adult and embryo by heart-derived progenitor cells. *Ann N Y Acad Sci*. 2004;1015:182–189.
30. Beltrami AP, Barlucchi L, Torella D, Baker M, Limana F, Chimenti S, Kasahara H, Rota M, Musso E, Urbanek K, Leri A, Kajstura J, Nadal-Ginard B, Anversa P. Adult cardiac stem cells are multipotent and support myocardial regeneration. *Cell*. 2003;114:763–776.
31. Laugwitz KL, Moretti A, Lam J, Gruber P, Chen Y, Woodard S, Lin LZ, Cai CL, Lu MM, Reth M, Platoshyn O, Yuan JX, Evans S, Chien KR. Postnatal isl1+ cardioblasts enter fully differentiated cardiomyocyte lineages. *Nature*. 2005;433:647–653.
32. He JQ, Ma Y, Lee Y, Thomson JA, Kamp TJ. Human embryonic stem cells develop into multiple types of cardiac myocytes: action potential characterization. *Circ Res*. 2003;93:32–39.
33. Sperger JM, Chen X, Draper JS, Antosiewicz JE, Chon CH, Jones SB, Brooks JD, Andrews PW, Brown PO, Thomson JA. Gene expression patterns in human embryonic stem cells and human pluripotent germ cell tumors. *Proc Natl Acad Sci U S A*. 2003;100:13350–13355.
34. Civin CI, Almeida-Porada G, Lee MJ, Olweus J, Terstappen LW, Zanjani ED. Sustained, retransplantable, multilineage engraftment of highly purified adult human bone marrow stem cells in vivo. *Blood*. 1996;88: 4102–4109.
35. Terstappen LW, Huang S, Safford M, Lansdorp PM, Loken MR. Sequential generations of hematopoietic colonies derived from single nonlineage-committed cd34+cd38- progenitor cells. *Blood*. 1991;77: 1218–1227.
36. Gekas C, Dieterlen-Lievre F, Orkin SH, Mikkola HK. The placenta is a niche for hematopoietic stem cells. *Dev Cell*. 2005;8:365–375.
37. James PR. A review of peripartum cardiomyopathy. *Int J Clin Pract*. 2004;58:363–365.
38. Mehta NJ, Mehta RN, Khan IA. Peripartum cardiomyopathy: Clinical and therapeutic aspects. *Angiology*. 2001;52:759–762.
39. Ro A, Frishman WH. Peripartum cardiomyopathy. *Cardiol Rev*. 2006; 14:35–42.
40. Bolli P, Chaudhry HW. Molecular physiology of cardiac regeneration. *Ann N Y Acad Sci*. 2010;1211:113–126.
41. Orlic D, Kajstura J, Chimenti S, Jakoniuk I, Anderson SM, Li B, Pickel J, McKay R, Nadal-Ginard B, Bodine DM, Leri A, Anversa P. Bone marrow cells regenerate infarcted myocardium. *Nature*. 2001;410: 701–705.
42. Nussbaum J, Minami E, Laflamme MA, Virag JA, Ware CB, Masino A, Muskheli V, Pabon L, Reinecke H, Murry CE. Transplantation of undifferentiated murine embryonic stem cells in the heart: teratoma formation and immune response. *FASEB J*. 2007;21:1345–1357.
43. van Laake LW, Passier R, Monshouwer-Kloots J, Verkleij AJ, Lips DJ, Freund C, den Ouden K, Ward-van Oostwaard D, Korving J, Tertoolen LG, van Echteld CJ, Doevendans PA, Mummery CL. Human embryonic stem cell-derived cardiomyocytes survive and mature in the mouse heart and transiently improve function after myocardial infarction. *Stem Cell Res*. 2007;1:9–24.
44. Xu C, Police S, Rao N, Carpenter MK. Characterization and enrichment of cardiomyocytes derived from human embryonic stem cells. *Circ Res*. 2002;91:501–508.
45. Yang L, Soonpaa MH, Adler ED, Roepke TK, Kattman SJ, Kennedy M, Henckaerts E, Bonham K, Abbott GW, Linden RM, Field LJ, Keller GM. Human cardiovascular progenitor cells develop from a kdr+ embryonic-stem-cell-derived population. *Nature*. 2008;453:524–528.
46. Martin CM, Meeson AP, Robertson SM, Hawke TJ, Richardson JA, Bates S, Goetsch SC, Gallardo TD, Garry DJ. Persistent expression of the ATP-binding cassette transporter, abcg2, identifies cardiac sp cells in the developing and adult heart. *Dev Biol*. 2004;265:262–275.
47. Wu SM, Chien KR, Mummery C. Origins and fates of cardiovascular progenitor cells. *Cell*. 2008;132:537–543.
48. Koyanagi M, Brandes RP, Haendeler J, Zeiher AM, Dimmeler S. Cell-to-cell connection of endothelial progenitor cells with cardiac myocytes by nanotubes: a novel mechanism for cell fate changes? *Circ Res*. 2005; 96:1039–1041.
49. Chawengsaksophak K, de Graaff W, Rossant J, Deschamps J, Beck F. Cdx2 is essential for axial elongation in mouse development. *Proc Natl Acad Sci U S A*. 2004;101:7641–7645.
50. Beck F, Stringer EJ. The role of Cdx genes in the gut and in axial development. *Biochem Soc Trans*. 2010;38:353–357.

51. Chawengsaksophak K, James R, Hammond VE, Kontgen F, Beck F. Homeosis and intestinal tumours in Cdx2 mutant mice. *Nature*. 1997; 386:84–87.
52. Ralston A, Rossant J. Genetic regulation of stem cell origins in the mouse embryo. *Clin Genet*. 2005;68:106–112.
53. Ralston A, Cox BJ, Nishioka N, Sasaki H, Chea E, Rugg-Gunn P, Guo G, Robson P, Draper JS, Rossant J. Gata3 regulates trophoblast development downstream of tead4 and in parallel to cdx2. *Development*. 2010;137:395–403.
54. Tanaka S, Kunath T, Hadjantonakis AK, Nagy A, Rossant J. Promotion of trophoblast stem cell proliferation by fgf4. *Science*. 1998;282:2072–2075.

Novelty and Significance

What Is Known?

- Microchimerism is the result of 2 genetically distinct populations of cells that appear in the same tissue, organ, or individual.
- Fetal cells can enter maternal blood and tissues and persist for decades as microchimeras.
- Fetal maternal transfer of cells can involve multiple cell types, some with regenerative properties, but this phenomenon had not been previously explored in acute cardiac injury.

What New Information Does This Article Contribute?

- Fetal cells selectively home to sites of cardiac injury and not to noninjured sites within the heart nor to noninjured organs; these fetal cells subsequently differentiate into diverse cardiac cell types.
- Fetal cells isolated from the maternal heart can form vascular tubes and spontaneously beating cardiomyocytes in vitro.
- Although these fetal cells are a heterogeneous mix of pluripotent cells, *Cdx2* is a highly prevalent marker amongst the fetal cells that home to the injured heart.

It has been reported that women with peripartum cardiomyopathy enjoy a high rate (~50%) of spontaneous recovery. This prompted us to hypothesize that there might be a fetal or placental contribution to maternal cardiac repair. Although our mouse injury model cannot precisely represent peripartum cardiomyopathy, it is a model of fetal maternal cell transfer which we believe may have identified appropriate cell types for cardiac regeneration. We induced mid-gestation myocardial infarction in pregnant female mice and euthanized them at various time points. Cells of fetal origin, marked by green fluorescent protein, homed to the injured areas of the heart but not to noninjured areas. They did not home to noninjured organs within the mouse either, and this suggests that precise signals are "sensed" by the fetal cells which enable them to target diseased tissue specifically. On homing to the heart, they differentiated into diverse cardiac lineages, including endothelial cells, smooth muscle cells, and cardiomyocytes. In vitro analysis of fetal cells isolated from maternal hearts demonstrated that they can recapitulate these differentiation pathways, forming vascular tubes in a 3D collagen matrix and spontaneously beating cardiomyocytes when co-cultured with neonatal cardiomyocytes. Although fetal cells isolated from maternal heart express a variety of pluripotency markers, a notable new finding was the finding that ~40% of these cells expressed Caudal-related homeobox2 (*Cdx2*), previously associated with trophoblast stem (TS) cells and other aspects of non-cardiac development. This knowledge will spur further investigations into a potential role for TS cells in cardiac regeneration and further studies of the signaling mechanisms of cells that "naturally" home to the diseased heart.

SUPPLEMENTAL MATERIAL

METHODS

Animals

WT female virgin mice on a B6CBA background and eGFP transgenic male mice on a C57Bl/6 background were purchased from Jackson Laboratories (Bar Harbor, MA). All mice used were between the ages of 3-6 months. All animal care was in compliance with the *Guide for the Care and Use of Laboratory Animals* published by the US National Institutes of Health, as well as institutional guidelines at Mount Sinai's School of Medicine. Initially, approximately 50 mice underwent LAD ligation surgery in order to determine the best time to induce injury. Embryonic day (E) 12 was chosen, as an earlier time point would cause the mother to resorb the embryos due to the hypoxic insult. If the injury was induced later in gestation, the pregnant mouse dies due to the hemodynamic consequences of the volume overload state in late pregnancy. Once it was determined that E12 was the best time to induce injury, the survival rate was 70%. The deaths that did occur were likely due to the infarction surgery and this survival rate matches our previously published results in non-pregnant mice [1].

Real-time Quantitative PCR

Quantitative PCR reactions were performed with iQ (SYBR Green Supermix) on the iQ5 Real-Time PCR Detection System (Bio-Rad, Hercules, CA). The PCR protocol consisted of one cycle at 95°C (10 minutes) followed by 40 cycles of 95°C (15 seconds) and 60°C (1 minute). Fold changes in gene expression were determined using the comparative CT method (ΔΔCt method) [2] with normalization to ApoB endogenous control. Primers used for RT-PCR experiments are as follows:

GFP-forward 5'-CATCGAGCTGAAGGGCATC-3',

GFP-reverse 5'-TGTTGTGGCGGATCTTGAAG-3',

ApoB-forward 5'-AAGGCTCATTTTCAACAATTCC-3',

ApoB-reverse 5'-GGACACAGACAGACCAGAAC-3',

Nkx2.5-forward 5'-GACAGGTACCGCTGTTGCTT-3'

Nkx2.5-reverse 5'-AGCCTACGGTGACCCTGAC-3',

GAPDH-forward 5'-CAGCAACAGGGTGGTGGAC-3',

GAPDH-reverse 5'-GGATGGAAATTGTGAGGGAGATG-3'

Comparative CT method (ΔΔCt method)

Briefly, the threshold cycle number (C_T) was obtained as the first cycle at which a statistically significant increase in fluorescence signal was detected. Data was normalized by subtracting the C_T value of ApoB from that of the eGFP. Each reaction was done in triplicate and the C_T values were averaged. The $\Delta\Delta C_T$ was calculated as the difference of the normalized C_T values (ΔC_T) of the treatment and control samples: $\Delta\Delta C_T = \Delta C_{T\ treatment} - \Delta C_{T\ control}$. $\Delta\Delta C_T$ was converted to fold of change by the following formula: fold of change = $2^{-\Delta\Delta CT}$ [2]. The fold differences in gene expression are represented as the mean ± SD. A minimum of three samples were run for each group at each time point (n=8 for experimental group at 1 week, n=5 at 2 weeks; n=3 for shams at 1 and 2 weeks; n=4 for non-infarcted control at 1 week, n=5 at 2 weeks). The fold-differences calculated using the $\Delta\Delta C_T$ method are usually expressed as a range, which is a result of incorporating the error of the $\Delta\Delta C_T$ value into the fold difference calculation. The error bars represent the top and bottom range of the fold-difference. P-values were determined by a two-tailed paired Student's t test from the ΔC_T values.

Absolute quantitation method

Q-PCR was performed utilizing genomic DNA extracted from whole hearts. A sensitivity test [3 4] was performed by mixing serial dilutions of DNA from GFP transgenic mouse hearts with each of three quantities of DNA from virgin female WT mouse hearts (0, 10,000, and 100,000 pg) and real-time

PCR for amplification of GFP was performed. 1 GFP cell amongst 100,000 cells of WT background can be detected. GFP is present as two copies per cell in the transgenic mouse we are utilizing [5] (See supplemental table 1 legend for detailed description).

Immunofluorescence

Maternal heart ventricular 4-μm-thick sections were fixed for 20 minutes and then blocked with 10% donkey serum (Jackson Immunoresearch, West Grove, PA) for 1h at room temperature (RT). Each section was incubated with the primary antibody for 1 hr at RT, followed by a secondary antibody for an additional 1 h at RT and counterstained with DAPI. Finally the sections were incubated for 5 minutes with Sudan Black (0.7% in 70% EtOH) and cover-slipped with mounting media (DAKO, Carpinteria, CA). Slides were imaged using a Zeiss LSM-510 Meta confocal microscope (Carl Zeiss, Munich Germany). The following primary antibodies were used for staining: rabbit anti-GFP (ABCAM #AB6556, Cambridge, MA), mouse anti-alpha sarcomeric actin (Sigma #A2172, St. Louis, MO), mouse anti-alpha sarcomeric actinin (Santa Cruz #15335, Santa Cruz, CA), mouse anti-cardiac troponin-T (ABCAM #AB45932), mouse anti-alpha-smooth muscle actin (Sigma #A2547), mouse anti-smooth muscle myosin IgG (Biomedical Technologies Inc #BT562, Stoughton, MA), rat anti-CD31 (BD #553370, San Jose, CA), rat anti-VE-Cadherin (RDI #RDI-MCD144-11D4, Acton, MA). Alexa-488 and Alexa-568 secondary antibodies were purchased from Molecular Probes (Invitrogen, Carlsbad, CA).

Isolation of Maternal Cardiac Cells

Chest wall was opened to expose heart which was perfused with 10mL PBS, using a 23-gauge needle. Entire heart was dissected out (atria and ventricle) and extraneous tissue removed. Small amounts of serum-free medium (DMEM, Cellgro, Manassas, VA) was added to prevent heart from drying out. Hearts from 3-4 adult mice were minced and placed in serum-free medium. Tissue was digested with pronase at 1mg/ml (Calbiochem, Gibbstown, NJ) in a spinning incubator for 1 h at

37°C. Supernatant was removed and 5mL of warm (37°C) complete medium (DMEM supplemented with 10% fetal bovine serum [Cellgro, Manassas, VA]) was added to the tube. (NOTE: No glycine was necessary to inactivate the pronase, as the serum in the medium does this). Skeletal/cardiac muscle was triturated in the medium. During trituration, small aliquots of tendon-free solution were transferred to an empty 50mL tube. Above procedure was repeated by adding 5mL aliquots of medium to the tube every few triturations until a final tendon-free volume of 35-45mL was achieved. Solution was filtered through a 70 micron mesh filter to remove small pieces of tendon. Filtered solution was spun at 3000rpm for 5 minutes. Pellet was resuspended in 3mL of medium then 21mL of red blood cell (RBC) lysis buffer (Ebiosciences, San Diego, CA) was added. After inverting a few times, filtered solution was spun at 3000 rpm for 5 min. Supernatant was removed and the pellet was resuspended in 1mL 1x PBS with antibiotics. Cells were counted.

FACS

Cells were sorted utilizing a MoFlo high speed cell sorter (Dako Cytomation, Carpinteria CA). Both eGFP+ (cells of fetal origin) and eGFP- (cells of maternal origin) populations were collected. Data analysis was performed using FlowJo Software (Tree Star, Ashland, OR).

Flow Cytometry Cell Analysis

Analysis of specific cell markers on previously sorted eGFP+ cells was performed utilizing the BD LSR II (BD Biosciences, San Jose, CA). For intracellular cell markers cells were permeabilized using Triton-X prior to antibody staining. The following antibodies were used for staining: anti-Sca1 (ebiosciences #17-5981-81), anti-c-kit (ebiosciences #27-1171-81), anti-oct4 (ebiosciences #12-5841-80), anti-nanog (ebiosciences #51-5761-80), anti-sox2 (Millipore #MAB4343, Billerica, MA), Islet1 (Hybridoma bank #39.4D5-s, Iowa City, IO), anti-nkx2.5 (Santa Cruz #sc-14033), anti-CD31 (Santa Cruz #sc-1506), anti-CD34 (ebiosciences #56-0341-82), anti-cdx2 (Santa Cruz #19478).

Cell Culture

- Differentiation of eGFP+ cells into endothelial cells and smooth muscle cells

CMFs were prepared by isolating cardiac cells from 1 day old WT neonatal pups. Cells were enriched for CMFs by spinning at low speeds (800 rpm). The supernatant (which primarily contains CMFs) was plated for 1 hour on culture dishes to allow CMFs to attach. The supernatant, now containing residual cardiomyocytes, was discarded. CMFs were incubated at 37ºC until confluent. CMFs were treated with Mitomycin C (MP Biomedicals. Solon, OH) to inhibit proliferation, incubated at 37ºC in complete medium for 24 hours and then used as feeders. FACS sorted eGFP+ cells were cultured on the CMFs and monitored for a period of 3-4 weeks. Live cell imaging was performed using an Olympus IX-70 Live cell imaging system (Olympus, Center Valley PA).

- Differentiation of eGFP+ cells into cardiomyocytes

Cardiomyocyte feeders were prepared by isolating cardiac cells from 1 day old cyclin A2 transgenic mice as these cardiomyocytes can be passaged and remain viable in culture indefinitely. Cells were enriched for cardiomyocytes by spinning at low speeds (800 rpm). The pellet (which primarily contains cardiomyocytes) was resuspended in complete medium and plated on culture dishes to allow residual CMFs to attach. The supernatant containing the cardiomyocytes was transferred to a new culture dish and then incubated at 37ºC. Feeders were ready for experiments after 24 hours. EGFP+ cells were cultured on cardiomyocyte feeders and monitored over a 4-5 week period. Live cell imaging was performed using an Olympus IX-70 Live cell imaging system (Olympus, Center Valley PA).

- Immunofluorescence

Cells were cultured in chamber slides for 4-5 weeks and fixed with 4% paraformaldehyde (PFA) for 20 minutes and then stained. Cells were incubated with primary antibody for 1 hour at RT, washed

three times and then incubated with a secondary antibody for an additional hour at room temperature. After staining, the cells were washed three times, cover-slipped with Dako mounting media and fluorescence was visualized using a Zeiss Axiophot2 fluorescence microscope (Carl Zeiss, Munich Germany).

- Clonal Assay

Single eGFP+ cells isolated from injured maternal hearts were seeded in 96-well plates containing feeders (cardiomyocytes or CMFs) with complete medium. The FACS Aria BCL2 (BD Biosciences, San Jose, CA) was utilized to sort single eGFP+ cells into 96 well plates. Cells were monitored daily to assay clonal expansion. Medium was changed every 3 days. After 14 days in culture, cells were fixed using 4% PFA and subjected to analysis.

Spectral Profile

Spectral scanning was performed using a Leica Microsystems (Leica, Mannheim, Germany) TCS SP5 confocal microscope. Images were collected using the lambda scan mode from 545nm-705nm with a 10nm bandwidth per image. The 543nm HeNe laser was used for excitation and images were collected at 512 x 512 pixels using the 63x/1.4NA HCX PL APO oil lens. Regions of interest (ROIs) were selected around both sample and control cells. The mean intensity vs. wavelength for each respective ROI was then plotted on a graph and compared to the Alexa Fluor 568 spectral profile.

XY Chromosome Analysis

To prepare the slide containing interphase nuclei for FISH analysis, it was first rinsed in 2xSSC/0.1%NP-40 for 2 min at room temperature. The slide was then dehydrated in an ethanol series and air-dried. Ready to Use (RTU) whole chromosome paint (WCP) mouse DNA probes for chromosomes X and Y (Cambio Ltd., Cambridge, UK) were mixed together and added to the slide. The interphase nuclei and probe were co-denatured for 5 minutes at 73ºC and hybridized for 48

hours at 37ºC. The slide was then washed, to remove non-bound probe, in 0.4xSSC/0.3%NP-40 for 2 min at 72ºC and 2xSSC/0.1%NP-40 for 2 min at room temperature and air-dried. The slide was mounted with a coverslip using DAPI II/Anti-fade (Abbott Molecular, Des Plaines, Illinois). Images were obtained using Zeiss Axioplan 2 fluorescent microscope with CytoVision software (Genetix Corp,San Jose, CA). Cy3- Orange, Absorption Max->550nm, Fluorescence Max->570nm, FITC-Green, Absorption Max->494nm, Fluorescence Max->520nm.

TaqMan Array for Pluripotent Genes

TaqMan® Array Gene Signature plates (Applied Biosystems, Carlsbad, CA) contain 92 assays to stem cell associated genes. Total RNA was extracted from FACS isolated eGFP+ cells from placenta. Relative gene expression was determined using a two-step quantitative real-time PCR according to the manufacturer's instructions.

1. Cheng RK, Asai T, Tang H, Dashoush NH, Kara RJ, Costa KD, Naka Y, Wu EX, Wolgemuth DJ, Chaudhry HW. Cyclin a2 induces cardiac regeneration after myocardial infarction and prevents heart failure. *Circ Res*. 2007;100:1741-1748
2. Pfaffl MW. A new mathematical model for relative quantification in real-time rt-pcr. *Nucleic Acids Res*. 2001;29:e45
3. Fujiki Y, Johnson KL, Tighiouart H, Peter I, Bianchi DW. Fetomaternal trafficking in the mouse increases as delivery approaches and is highest in the maternal lung. *Biol Reprod*. 2008;79:841-848
4. Su EC, Johnson KL, Tighiouart H, Bianchi DW. Murine maternal cell microchimerism: Analysis using real-time pcr and in vivo imaging. *Biology of reproduction*. 2008;78:883-887
5. Joshi M, Keith Pittman H, Haisch C, Verbanac K. Real-time pcr to determine transgene copy number and to quantitate the biolocalization of adoptively transferred cells from egfp-transgenic mice. *BioTechniques*. 2008;45:247-258

ONLINE TABLES

Online Table I: Absolute quantification of GFP cells in whole hearts of pregnant female mice mated with GFP-transgenic males. Standard curves were generated for both GFP and ApoB by plotting C_T values for different quantities of known amounts of DNA from GFP transgenic mice versus the DNA quantity in ng. The equations that fit these curves are presented above. In the first row, data for the 2 weeks time point are presented; in the second row, data for the 1 week time point are presented. Column A represents time point; Column B represents sample type; Column C depicts C_T value (in triplicate averaged over 3 mice) for each sample; Column D represents the DNA quantity as extrapolated from the GFP standard curve for each experimental C_T value; Column E is the DNA quantity as extrapolated from the ApoB standard curve; Column F is the ratio of values in E/values in D (normalizing to ApoB expression levels as described in learn.appliedbiosystems.com); Column G represents the inverse log of values in F to derive 'normalized' DNA quantity; Column H is the DNA quantity converted to pg; Column I is the number of GFP cells in that sample of DNA utilizing the mouse genome conversion factor for this strain of mouse as referred to in Fujiki et al., Biol Reprod, 2008 and Column J represents the absolute percentage of GFP cells in the whole heart- 1.3% cells of whole heart are GFP-positive at 1 week post-injury and 1.7% cells of whole heart are GFP-positive at 2 weeks post-injury.

A	B	C	D	E	F	G	H	I	J
Time point	**Sample**	**CT**	**X_{GFP}=Y-35.867/-2.584**	**X_{ApoB}=Y-30.541/-3.7324**	**X_{ApoB}/X_{GFP} {log DNA (ng)}**	**DNA (ng)**	**DNA (pg)**	**Cell #s (6.25pg DNA/cell)**	**%Cell #s/heart**
2 wks post MI	No MI	33.6	0.877321981	-0.819579895	-0.9341837	0.116363372	116.3633725	19.39389542	0.121211846
	Sham	32.5	1.303018576	-0.524863359	-0.402805738	0.395543509	395.5435093	65.92391821	0.412024489
	MI	28	3.044504644	0.680795199	0.223614439	1.673456544	1673.456544	278.9094241	1.7431839
1wk post MI	No MI	35.00	0.335526316	-1.194673668	-3.560596031	0.000275045	0.275045136	0.045840856	0.000286505
	Sham	33.45	0.935371517	-0.779391276	-0.833242473	0.146810638	146.8106382	24.4684397	0.152927748
	MI	29.67	2.398219814	0.233361912	0.097306306	1.251141144	1251.141144	208.5235241	1.303272025
			GFP Standard Curve Equation	**ApoB Standard Curve Equation**					
			y = -2.584x + 35.867	y = -3.7324x + 30.541					
			R^2 = 0.994	R^2 = 0.9867					

Online Table II: Cell quantification in ventricular tissue sections obtained from WT female mice mated with GFP transgenic mice, subjected to cardiac injury at mid-gestation, then sacrificed 3 weeks post-injury. 10 different sections in infarct zones and 10 different sections in non-infarct zones that comprised an area of 25 sq. mm each were utilized for this analysis. All nuclei (detected by DAPI staining) were counted in each section. All eGFP+ nuclei were also counted and the ratios are presented in Table 2A. This was repeated in non-infarct zones and the ratios are presented in Table 2B. Alpha-actinin stained cells were counted in the infarct zones (mononuclear) and the ratio of eGFP+ nuclei that were present in alpha-actinin stained cells is presented in Table 2C.

A	Total nuclei infarct zone	eGFP+ nuclei	% eGFP+/total nuclei
1	64	6	9.3
2	81	3	3.7
3	112	3	2.7
4	123	2	1.6
5	81	3	3.7
6	105	4	3.8
7	127	1	0.8
8	71	1	1.4
9	85	1	1.2
10	79	2	2.5
B	**Total nuclei Non-infarct zone**	**eGFP+ nuclei Non-Infarct Zone**	**%eGFP+ nuclei Non-Infarct Zone**
1	72	1	1.4
2	93	0	0
3	84	0	0
4	101	0	0
5	147	0	0
6	62	1	1.6
7	55	0	0
8	80	0	0
9	81	0	0
10	64	0	0
Avg	**83.9**	**0.2**	**0.2**
C	**Total eGFP+ nuclei**	**eGFP+ Actinin+ nuclei**	**% eGFP+ Actinin+/eGFP nuclei**
1	6	4	66.7
2	3	1	33.3
3	3	2	66.7
4	2	1	50
5	3	1	33.3
6	4	2	50
7	1	0	0
8	1	0	0
9	1	0	0
10	2	2	100
Avg	**2.6**	**1.3**	**50**

Online Table III: Complete list of gene expression results from eGFP+ cells isolated from late term placenta, using Taqman array mouse stem cell pluripotency 96-well plate (Part Number 4414080).

	Raw Ct Values			Values Normalized to Gapdh		
Gene ID	**Placenta1**	**Placenta2**	**Placenta3**	**Placenta1**	**Placenta2**	**Placenta3**
18S-Hs99999901_s1	6.3705	8.47053	16.0094			
Gapdh-Mm99999915_g1	20.9696	18.8751	13.6232	0	0	0
Hprt1-Mm00446968_m1	25.9639	23.6467	33.147	4.9943	4.7716	19.5238
Gusb-Mm00446953_m1	26.4595	24.424	33.4364	5.4899	5.5489	19.8132
Actc1-Mm01333821_m1	28.8881	25.4953	22.127	7.9185	6.6202	8.5038
Afp-Mm00431715_m1	20.0476	18.6008	12.1797	-0.922	-0.2743	-1.4435
Bxdc2-Mm00503229_m1	27.1527	24.3709	20.021	6.1831	5.4958	6.3978
Cd34-Mm00519283_m1	26.2739	23.7997	18.4277	5.3043	4.9246	4.8045
Cd9-Mm00514275_g1	24.2361	21.3352	17.3176	3.2665	2.4601	3.6944
Cdh5-Mm00486938_m1	23.3841	20.926	15.4999	2.4145	2.0509	1.8767
Cdx2-Mm00432449_m1	27.8661	27.2999	21.1473	6.8965	8.4248	7.5241
Col1a1-Mm00801666_g1	20.7192	18.2277	13.2472	-0.2504	-0.6474	-0.376
Col2a1-Mm00491889_m1	26.1934	27.0833	19.0532	5.2238	8.2082	5.43
Commd3-Mm00521684_m1	30.2898	27.3424	24.3104	9.3202	8.4673	10.6872
Crabp2-Mm00801693_g1	29.5281	27.8679	22.113	8.5585	8.9928	8.4898
Ddx4-Mm00802445_m1	33.419	31.4264	27.0787	12.4494	12.5513	13.4555
Des-Mm00802455_m1	27.1446	26.0115	20.7865	6.175	7.1364	7.1633
Dnmt3b-Mm01240113_m1	29.001	27.4062	22.5412	8.0314	8.5311	8.918
Lefty1-Mm00438615_m1	Undetermined	36.3593	31.8521	Undetermined	17.4842	18.2289
Eomes-Mm01351985_m1	34.1758	32.7162	27.0058	13.2062	13.8411	13.3826
Fgf4-Mm00438917_m1	Undetermined	Undetermined	Undetermined	Undetermined	Undetermined	Undetermined
Fgf5-Mm00438919_m1	35.3186	36	30.7142	14.349	17.1249	17.091
Flt1-Mm00438980_m1	26.067	24.1073	19.1198	5.0974	5.2322	5.4966
Fn1-Mm01256744_m1	21.7467	19.7424	14.3723	0.7771	0.8673	0.7491
Foxa2-Mm01976556_s1	28.0793	25.4683	25.0441	7.1097	6.5932	11.4209
Foxd3-Mm02384867_s1	Undetermined	30.8118	Undetermined	Undetermined	11.9367	Undetermined
Gabrb3-Mm00433473_m1	35.8833	32.5907	28.297	14.9137	13.7156	14.6738
Gal-Mm00439056_m1	33.0773	29.2917	24.8623	12.1077	10.4166	11.2391
Gata4-Mm00484689_m1	26.0794	25.4503	19.0996	5.1098	6.5752	5.4764
Gata6-Mm00802636_m1	26.988	24.3801	19.2929	6.0184	5.505	5.6697
Gbx2-Mm00494578_m1	Undetermined	31.4816	27.8815	Undetermined	12.6065	14.2583
Gcg-Mm00801712_m1	Undetermined	38.1937	33.0883	Undetermined	19.3186	19.4651
Gcm1-Mm00492310_m1	31.5349	31.052	23.4502	10.5653	12.1769	9.827
Gdf3-Mm00433563_m1	36.7057	34.4247	29.3908	15.7361	15.5496	15.7676
Gfap-Mm00546086_m1	36.3519	35.458	28.0648	15.3823	16.5829	14.4416
Grb7-Mm01306734_m1	28.2935	26.5652	21.7775	7.3239	7.6901	8.1543
Hbb-b2-Mm00731743_mH	20.7765	20.2892	13.2353	-0.1931	1.4141	-0.3879
Hba-x-Mm00439255_m1	23.6843	25.7335	16.204	2.7147	6.8584	2.5808
Mnx1-Mm00658300_g1	37.833	33.6542	29.1002	16.8634	14.7791	15.477
Iapp-Mm00439403_m1	Undetermined	Undetermined	34.065	Undetermined	Undetermined	20.4418
Ifitm1-Mm00850040_g1	26.5783	23.0079	21.176	5.6087	4.1328	7.5528
Ifitm2-Mm00850080_g1	27.9784	24.3113	24.372	7.0088	5.4362	10.7488
Il6st-Mm00439668_m1	26.2689	24.1603	19.5894	5.2993	5.2852	5.9662
Igfbp2-Mm00492632_m1	26.9526	25.3066	20.1445	5.983	6.4315	6.5213

Ins2-Mm00731595_gH	Undetermined	30.2597	28.4544	Undetermined	11.3846	14.8312
Pdx1-Mm00435565_m1	Undetermined	35.5069	31.2635	Undetermined	16.6318	17.6403
Isl1-Mm00627860_m1	38.4946	33.7686	28.5575	17.525	14.8935	14.9343
Kit-Mm00445212_m1	26.2121	25.2267	19.107	5.2425	6.3516	5.4838
Krt1-Mm00492992_g1	30.9432	33.8954	24.0382	9.9736	15.0203	10.415
Lama1-Mm00439445_m1	23.3831	23.2048	15.6915	2.4135	4.3297	2.0683
Lamb1-1-Mm00801853_m1	24.1153	21.8563	16.8898	3.1457	2.9812	3.2666
Lamc1-Mm00711820_m1	23.7416	21.9146	16.7137	2.772	3.0395	3.0905
Lefty2-Mm00774547_m1	Undetermined	37.5112	30.8274	Undetermined	18.6361	17.2042
Lifr-Mm00442940_m1	24.8734	23.0875	17.5635	3.9038	4.2124	3.9403
Lin28-Mm00524077_m1	30.6329	30.7133	23.7301	9.6633	11.8382	10.1069
Myf5-Mm00435125_m1	Undetermined	Undetermined	Undetermined	Undetermined	Undetermined	Undetermined
Myod1-Mm00440387_m1	36.7214	33.2402	33.0302	15.7518	14.3651	19.407
Nanog-Mm02019550_s1	37.0344	26.5706	27.9819	16.0648	7.6955	14.3587
Nes-Mm00450205_m1	28.063	27.425	21.2942	7.0934	8.5499	7.671
Neurod1-Mm01946604_s1	Undetermined	28.183	30.9275	Undetermined	9.3079	17.3043
Nodal-Mm00443040_m1	33.4446	32.016	26.1958	12.475	13.1409	12.5726
Nog-Mm00476456_s1	27.4575	25.9114	20.7441	6.4879	7.0363	7.1209
Nppa-Mm01255747_g1	35.4623	33.6554	29.1081	14.4927	14.7803	15.4849
Nr5a2-Mm00446088_m1	34.1867	33.3681	27.3547	13.2171	14.493	13.7315
Nr6a1-Mm00599848_m1	30.1965	28.0504	23.2667	9.2269	9.1753	9.6435
Olig2-Mm01210556_m1	36.607	37.1301	29.3012	15.6374	18.255	15.678
Pax4-Mm01159036_m1	Undetermined	Undetermined	Undetermined	Undetermined	Undetermined	Undetermined
Pax6-Mm00443072_m1	36.5576	34.7341	30.4868	15.588	15.859	16.8636
Pecam1-Mm00476702_m1	24.4944	22.4209	17.2251	3.5248	3.5458	3.6019
Podxl-Mm00449829_m1	24.7904	24.0435	17.0374	3.8208	5.1684	3.4142
Pou5f1-Mm00658129_gH	35.2662	32.652	29.28	14.2966	13.7769	15.6568
Pten-Mm00477210_m1	27.204	24.7365	20.3668	6.2344	5.8614	6.7436
Ptf1a-Mm00479622_m1	Undetermined	Undetermined	Undetermined	Undetermined	Undetermined	Undetermined
Rest-Mm00803268_m1	27.8035	25.3074	20.7451	6.8339	6.4323	7.1219
Runx2-Mm00501578_m1	Undetermined	36.1486	31.7123	Undetermined	17.2735	18.0891
Sema3a-Mm00436469_m1	32.1638	29.0252	25.3798	11.1942	10.1501	11.7566
Serpina1a-Mm02748447_g1	31.0904	26.3099	25.5911	10.1208	7.4348	11.9679
Sfrp2-Mm00485986_m1	29.387	26.3426	22.2145	8.4174	7.4675	8.5913
Sox17-Mm00488363_m1	27.3797	27.152	20.0432	6.4101	8.2769	6.42
Sox2-Mm00488369_s1	Undetermined	27.3828	26.4852	Undetermined	8.5077	12.862
Sycp3-Mm00488519_m1	36.7673	32.6623	29.1498	15.7977	13.7872	15.5266
Syp-Mm00436850_m1	33.0295	30.0902	24.2542	12.0599	11.2151	10.631
T-Mm00436877_m1	Undetermined	Undetermined	39.9782	Undetermined	Undetermined	26.355
Tat-Mm01244282_m1	35.7324	36.7088	30.4848	14.7628	17.8337	16.8616
Tdgf1-Mm00783944_g1	Undetermined	27.1602	28.2507	Undetermined	8.2851	14.6275
Tert-Mm00436931_m1	32.5026	30.957	26.0882	11.533	12.0819	12.465
Tcfcp2l1-Mm00470119_m1	31.0598	30.9915	24.7141	10.0902	12.1164	11.0909
Th-Mm00447546_m1	Undetermined	37.1873	30.4919	Undetermined	18.3122	16.8687
Utf1-Mm00447703_g1	31.1389	28.538	25.2141	10.1693	9.6629	11.5909
Wt1-Mm00460570_m1	31.4399	30.056	24.2453	10.4703	11.1809	10.6221
Xist-Mm01232884_m1	27.0304	24.1311	19.2598	6.0608	5.256	5.6366
Zfp42-Mm01194090_g1	29.3088	25.9252	23.1699	8.3392	7.0501	9.5467
Eras-Mm01345955_s1	Undetermined	28.1246	28.6338	Undetermined	9.2495	15.0106
Raf1-Mm00466513_m1	27.2131	25.4176	19.9228	6.2435	6.5425	6.2996
Ctnnb1-Mm00483033_m1	23.5056	21.6847	15.913	2.536	2.8096	2.2898
Eef1a1-Mm01966109_u1	19.9088	16.648	13.2675	-1.0608	-2.2271	-0.3557

Online Table IV: Real time q-PCR. Nkx2.5 gene expression in late term placenta of mouse with cardiac injury relative to positive control (E16.5 mouse heart)

Sample	CT	Average CT	STDEV	SEM	Average normalizer	Delta CT	Delta Delta CT	Fold change
Placenta-GAPDH	22.83313	22.699232	0.124194105	0.0717035	22.699232			
Placenta-GAPDH	22.587812							
Placenta-GAPDH	22.676754							
Heart-GAPDH	16.958006	16.905454	0.074624554	0.043084507	16.905454			
Heart-GAPDH	16.938318							
Heart-GAPDH	16.820038							
Placenta-Nkx2.5	39.856915	39.769009	0.124317857	0.071774948		17.069777	11.484933	0.000348892
Placenta-Nkx2.5	Undetermined							
Placenta-Nkx2.5	39.681103							
Heart-Nkx2.5	22.515194	22.490298	0.037273612	0.02151993		5.584844	0	1
Heart-Nkx2.5	22.447445							
Heart-Nkx2.5	22.508255							

Online Figure I: Negligible Nkx2.5 expression in late term placenta of mouse with cardiac injury relative to positive control (E16.5 heart). Nkx2.5 expression by q-PCR above was plotted relative to Nkx2.5 expression in E16.5 heart

Online Movie Legends

Online Movie I: live imaging of eGFP+ fetal cell #1 that has differentiated to a beating cardiomyocyte 4.5 weeks after culturing

Online Movie IA: live imaging of beating cardiomyocyte from Movie S1, without fluorescence so that syncytial beating with neighboring cells can be observed

Online Movie Still Image IB: still image of cardiomyocyte from Movie S1 to demonstrate eGFP+ fetal cell is adjacent to other cells that can be observed beating in Movie S1A

Online Movie II: live imaging of eGFP+ fetal cell #2 that has differentiated to a beating cardiomyocyte 4.5 weeks after culturing

Online Movie III: live imaging of eGFP+ fetal cell #3 that has differentiated to a beating cardiomyocyte 4.5 weeks after culturing